Increased Expression of Activating Factors in Large Osteoclasts Could Explain Their Excessive Activity in Osteolytic Diseases

Diana P. Trebec,[1]* Divya Chandra,[2] Azza Gramoun,[2] Keying Li,[2] Johan N.M. Heersche,[2] and Morris F. Manolson[1,2]

[1]Department of Biochemistry, Faculty of Medicine, University of Toronto, Toronto, Ontario, Canada
[2]Faculty of Dentistry, University of Toronto, Toronto, Ontario, Canada

Abstract   Large osteoclasts (≥ 10 nuclei) predominate at sites of pathological bone resorption. We hypothesized this was related to increased resorptive activity of large osteoclasts and have demonstrated previously that larger osteoclasts are 8-fold more likely to be resorbing than small osteoclasts (2–5 nuclei). Here we ask whether these differences in resorptive activity can be explained by differences in expression of factors involved in osteoclast signaling, fusion, attachment, and matrix degradation. Authentic rabbit osteoclasts and osteoclasts derived from RAW264.7 cells showed similar increases in c-fms expression (1.7- to 1.8-fold) in large osteoclasts suggesting that RAW cells are a viable system for further analysis. We found 2- to 4.5-fold increases in the expression of the integrins α_v and β_3, the proteases proMMP9, matMMP9 and pro-cathepsinK, and in activating receptors RANK, IL-1R1, and TNFR1 in large osteoclasts. In contrast, small osteoclasts had higher expression of the fusion protein SIRPα1 and the decoy receptor IL-1R2. The higher expression of activation receptors and lower expression of IL-1R2 in large osteoclasts suggest they are hyperresponsive to extracellular factors. This is supported by the observation that the resorptive activity in large osteoclasts was more responsive to IL-1β, and that this increased activity was inhibited by the IL-1 receptor antagonist, IL-1ra. This increased responsiveness of large osteoclasts to IL-1 may, in part, explain the pathological bone loss noted in inflammatory diseases. The heterogeneity in receptor expression and the differential response to cytokines and their antagonists could prove useful for selective inhibition of large osteoclasts actively engaged in pathological bone loss. J. Cell. Biochem. 101: 205–220, 2007. © 2007 Wiley-Liss, Inc.

Key words: bone; arthritis; inflammation; osteoclasts; cytokines

---

Osteoclasts (OC) are multinucleated cells whose primary function is the resorption of mineralized bone matrix. Depending on the species, OCs involved in normal bone remodeling contain on average 3–10 nuclei [Piper et al., 1992]. In disease states involving pathological bone loss such as inflammatory arthritis, periodontal disease and Paget's disease, large OCs predominate in the areas of excessive resorption [Arend and Dayer, 1990; Aota et al., 1996; Singer and Roodman, 1996; Smith et al., 1997]. In Paget's disease, OCs have been detected that were 100 μm in diameter and contained up to 100 nuclei [Singer and Roodman, 1996].

Several studies have investigated whether OC size is linked to resorptive activity. Piper et al. [1992] demonstrated a decrease in volume of resorption per nucleus as the number of nuclei per cell increased, while Lees et al. [2001] found that resorption per nucleus was not different between large (greater than 10 nuclei) and small OCs (containing 2–5 nuclei). Interestingly however, Lees et al. [2001] observed that approximately 40% of the large OCs were actively resorbing in the population while only ~6% of the small OCs were doing likewise. They

also found that intracellular pH was lower in resorbing cells than in non-resorbing ones and was lower in large OCs than in small ones [Lees and Heersche, 2000]. One of the essential enzymes in OC pH regulation is the proton pumping vacuolar-type ATPase (V-ATPase) [Nordstrom et al., 1997]. Manolson et al. [2003] showed that mRNA expression of the "a3" V-ATPase subunit in OCs derived from rabbit long bones, and protein expression in RAW-cell derived OCs was significantly increased in large compared to small OCs.

Based on the observation that the percentage of large OCs that is actively resorbing is 8 times greater than the percentage of small OCs actively resorbing when the cells are maintained in the same culture media [Lees et al., 2001], we hypothesize that differences in signaling receptor expression allow the cells to respond differently to activating factors within their environment. To test this hypothesis, we quantified the expression levels of receptors for interleukin-1 (IL-1), tumor necrosis factor-α (TNFα), Receptor activator of nuclear factor kappa-B ligand (RANKL) and monocyte/macrophage-colony stimulating factor (M-CSF), all key factors in the inflammatory response and implicated in OC activation. Additional factors found to be involved in OC activation, fusion and attachment were also investigated.

MATERIALS AND METHODS

Materials

The RAW 264.7 cell line (RAW) was obtained from American Type Culture Collection (ATCC catalog # TIB-71). Dulbecco's modified Eagle's medium, α-MEM, antibiotics (penicillin/streptomycin, fungizone) and sterile fetal bovine serum (GIBCO #12318-028) were obtained from Invitrogen. Antibodies to IL-1R1, TNFR1, c-fms, SIRPα1, and integrin β_3 were obtained from Santa Cruz, as were HRP conjugated secondary antibodies to mouse, rabbit and goat. Antibodies to RANK, and IL-1R2 were obtained from R&D Systems and integrin α_v from BD biosciences. Monoclonal antibody to GAPDH was obtained from Abcam, while those for MMP-9 and cathepsin K were kindly provided by Dr. John Mort (McGill). Antibody to SHIP was kindly provided by Dr. Gerald Krystal (University of British Columbia). Phosphatase Substrate (catalog #P4744-1G), p-nitrophenol (catalog # 104-8),

Fast Red Violet LB Salt (catalog # F-1625) and Naphtol AS-MX (catalog# N-5000) were obtained from Sigma.

In Situ Hybridization

Dispersed rabbit OCs used for in situ hybridization were obtained from dissected shafts of the femorae, tibiae, humeri and radii of 1-day-old New Zealand white rabbits as previously described [Kanehisa and Heersche, 1988; Lees and Heersche, 1999; Manolson et al., 2003].

Oligonucleotide PCR probes designed to encode rabbit c-fms (from Genbank accession numbers R86522, R86582, R86469, R86465) are as follows: sense 5'-gct cta gaa gtg gga gtt ccc ccg-3'; and antisense 5'-gac gtc gac ctc cag cag gaa agt tga gc-3'. Restriction sites to XbaI and SalI in the forward and reverse strands respectively were incorporated into the oligonucleotides. Template RNA was obtained from rabbit OCs using the mRNA Capture Kit (Boehringer Mannheim) as described in Manolson et al. [2003]. cDNA was generated using Superscript One Step PCR system (GibcoBRL) following manufacturers instructions and RT-PCR was performed as follows: 15 min at 45°C, 2 min at 94°C, followed by 40 cycles of 15 s at 94°C, 30 s at 60°C, 1 min at 68°C, and a final step of 5 min at 72°C. The resulting 313 bp cDNA fragment was cloned into XbaI and SalI sites of Bluescript (KS-) and sequenced. ^{35}S-labels were generated with plasmids for c-fms linearized with restriction enzymes at 3' and 5' ends. c-fms linearized with NotI overnight (O/N) at 37°C was used to generate the antisense probe and XhoI was used to obtain the sense strand. Linearized cDNA was phenol extracted and then used to synthesize the radiolabeled cRNA probe incorporating ^{35}S-UTP (1100 Ci/mmol) via an RNA labeling kit (Promega).

Labeled antisense and sense mRNA probes against c-fms were hybridized to OC mRNA. Single Stranded probe was resuspended in hybridization buffer (1$\times$ Denhardt's solution, 20 mM Tris pH 8.0, 5 mM EDTA, 10 mM phosphate pH 6.8, 50% deionized formamide, 10% dextran sulfate (as a 50% solution), 50 mM DTT, 500 μg/ml tRNA (Sigma) in ddH$_2$O, 50 μg/ml polyA RNA (BCL)) and heat denatured immediately before use with 50,000−100,000 cpm added per slide. Pretreatment of OCs on slides included 18 min in 0.2N HCl, 5 min 2$\times$ SSC and permeabilization for 7 min with 5 μg/ml proteinase K. Slides were immersed in 4%

paraformaldehyde in PBS for 15 min, followed by 10 min in acetic acid triethanolamine buffer. They were then washed once in PBS and once in ddH$_2$O, dehydrated using 30, 60, 80, and 95% ethanol, then air dried. Slides were incubated with probe O/N at 55°C in humidified chambers. After hybridization slides were washed in 2× SSC, 50% formamide, 10 mM DTT, RNase buffer, 0.1× SSC, dipped in NTB-2 Kodak emulsion (Amersham) at 42°C and subsequently stored in desiccated lightproof boxes at 4°C. After 3–14 days, the slides were developed for 4 min in Kodak D19 developer, rinsed with water and fixed for 5 min. Counterstaining of OCs was carried out using malachite green. In situ hybridization data was normalized by expressing the data on a per nucleus basis. This can easily be done, because in cells in culture, as opposed to histological sections from OCs in situ, the total number of cells can be counted accurately.

Silver grains per cell were quantified by light microscopy using Imagepro Plus 4.1 (media cybernetics, des Moines, Iowa). Quantification was performed on individual OCs and results expressed as grains/nucleus. Statistical analysis was performed using the unpaired, two-tailed Student's t-test.

Differentiation and Isolation of Large and Small OCs From the RAW 264.7 Cell Line

Populations of at least 75–80% large (≥10 nuclei) or 80–95% small (2–5 nuclei) OCs were obtained as described in [Manolson et al., 2003]. Culture dishes were visually inspected until at least 80% of the total nuclei were contained within small (2–5 nuclei) OCs (generally day 5) or until at least 75% of the total nuclei were within large (≥10 nuclei) OCs (generally day 8) as defined previously [Manolson et al., 2003]. Prior to protein and/or RNA isolation, remaining mononuclear cells were removed by gently washing the dishes with 3 × 10 ml phosphate buffered saline (PBS) without Ca^{2+} and Mg^{2+}.

Gradient Separation of Large and Small OCs

OCs were generated with 200 ng/ml sRANKL in 100 mm dishes as outlined above for 4–5 days until a mixed OC population was obtained. OCs were then separated on a FBS gradient as described by Collin-Osdoby et al. [2003] with the modifications detailed below. Briefly, dishes were washed in Moscona's High Bicarbonate buffer (MHB) pH 7.2 (137 mM NaCl, 2.68 mM KCl, 0.4 mM NaH$_2$PO$_4$, 12 mM NaHCO$_3$, 11 mM dextrose, with addition of antibiotic-antimycotic solution (Gibco# 15240-096)), then incubated at 37°C for 15 min in MHB. MHB was replaced with a collagenase-trysin solution in Hank's Balanced Salt Solution (Gibco#14175-095) for 5 min at 37°C, then washed 3× in PBS and a solution of protease (EC 3.4.24.31 sigma P-8811)-EDTA was added for 15–20 min at 37°C. Cells were then removed from the plate by gently pipetting over the monolayer of cells, with resulting suspensions collected and centrifuged at 100g for 5 min. Pellets were resuspended in MHB and added to the top of a 40%/70% step gradient of FBS in MHB and left to stand undisturbed for 30 min at room temperature. Three fractions were then removed and pelleted as described in Collin-Osdoby et al. [2003]. Large OCs were found in the "bottom" 12 ml fraction while small OCs remained in the "middle" 16 ml fraction. Cells were then either replated for TRAP staining and counting, or, to obtain protein, pellets were resuspended in serum-free DMEM to wash out excess FBS and repelleted by centrifuging once more at 100g for 5 min. Pellets were then resuspended in RIPA lysis buffer and protein obtained as described below for immunoblotting experiments.

Protein Isolation

Protein was harvested from RAW-cell derived OCs using three separate methods: TRIzol, RIPA, and octyl-β-D-glucoside, as some methods were found to yield better immunoblotting results for certain proteins under investigation. These methods are described below.

Cells were initially harvested using TRIzol reagent (Life Technologies) to isolate total RNA and protein from the cells, following manufacturer's instructions. RNA storing solution (Ambion) was used to dissolve RNA pellets at 4°C. Protein pellets were dissolved in 1% SDS.

The method used to isolate protein was later changed to obtain better yields. One such method employed RIPA buffer for isolation [50 mM Tris, 150 mM NaCl, 1% Triton-X, 1% SDS, 0.5% sodium deoxycholate]. Briefly, cells were washed with cold PBS-Mg^{2+}and -Ca^{2+}. Cells were then scraped into approximately 1 ml RIPA+ complete protease inhibitor cocktail (Roche) which were added to cell culture dishes.

The whole cell lysate was left on ice 20 min with vortexing, then centrifuged at ~14,000 rpm at 4°C, for 15 min. Protein concentrations were determined and then used to adjust the amounts for immunoblotting.

Octyl-β-D-glucoside was adopted for isolation of integrin proteins, following methodology adapted from Ha et al. [2003]. Briefly, cells were washed with cold PBS-$Mg^{2+}$and -Ca^{2+}. Cells were scraped into lysis buffer (TNE Buffer (20 mM Tris-HCl, pH 7.4, 150 mM NaCl, 1 mM EDTA) + 0.5% Brij 58, +60 mM Octyl Glucoside, and +0.3% sodium deoxycholate) including protease inhibitors. The whole cell lysate was incubated on ice for 1 h, and then centrifuged at 14,000 rpm for 30 min at 4°C. The soluble fraction was kept.

TRIzol extractions were found to work best for soluble factors MMP-9 and Cathepsin K. RIPA isolations were found to yield the best results for detection of RANK, IL-1R1, IL-1R2, TNFR1, SHIP, and SIRPα1, while detection for integrins was best using the octyl-β-D-glucoside protein isolation method.

Immunoblotting

Protein titrations from 5 to 100 μg were run on 8–10% mini SDS–PAGE gels. Protein was transferred to nitrocellulose (Amersham Hybond-ECL) using full immersion transfer apparatus (Bio-Rad) on ice at 75 V, 150 mAmps for 1 h (or 130 mAmps for 1.5 h). Transfer was confirmed by staining with 0.2% Ponceau-S in acetic acid. Blots were then blocked in Tris buffered saline Tween-20 (TBS-T) + 5% milk solution for 1 h. Primary antibodies were added at appropriate dilutions in TBS-T + 5% milk and the blots incubated at 4°C O/N. GAPDH was detected by probing with anti-GAPDH and was used as a control. Blots were then washed in TBS-T, after which appropriate secondary antibody was added at concentrations of 1:1,000–1:5,000 in TBS-T + milk incubated at room temperature for 1 h. Blots were then washed and developed using ECL reagents (Amersham Biosciences). Images were captured using GeneSnap (Syngene). Quantification and analysis were performed using GeneTools (Syngene) as previously described [Manolson et al., 2003]. Briefly, to ensure that the chemiluminescent signals from the immunoblots were within the linear range, each protein sample was run on the SDS–PAGE as a series of four serial dilutions. Multiple exposure times

were recorded using a CCD camera, and an exposure was used for quantification only if the obtained signal reflected the serial dilution of the sample. For each separate gel, the absolute value obtained at each of the four protein concentrations was divided by the absolute value obtained for GAPDH. GAPDH was used to normalize the signal between different samples as in situ hybridization had revealed no difference in GAPDH gene expression between large and small OCs [Manolson et al., 2003]. Receptor/GAPDH ratios were then plotted against μg of protein loaded per lane and a linear regression line was fitted using the method of least-squares. The slope of this linear regression line was then used to compare the relative expression of the various factors between different experiments.

Tartrate-Resistant Acid Phosphatase (TRAP) Staining

Culture dishes were washed with PBS-Ca^{2+} and -Mg^{2+}, then fixed with 2.5% gluteraldehyde for 5–10 min. Staining for TRAP was carried out according to the protocol described in BD Biosciences Technical Bulletin #445 with minor modifications. Briefly, TRAP staining solution consisting of 50 mM acetate buffer, 30 mM sodium tartrate, 0.1 mg/ml Naphtol AS-MX phosphate, 0.1% Triton X-100, and 0.3 mg/ml Fast Red Violet LB stain was added to fixed cells for 10–20 min until desired staining intensity was reached. TRAP solution was removed and cells were washed 3×10 ml with dH_2O.

TRAP Assay

Assay for TRAP enzyme activity was adapted from a Sigma protocol as previously described in Voronov et al. [2005]. Briefly, cells were lysed in citrate buffer containing 0.1% Triton X-100. Lysate was added to ELISA plates containing phosphatase substrate (p-nitrophenol phosphate) and 40 mM tartrate acid buffer and incubated at 37°C for 30 min. The reaction was then stopped with the addition of cold 2N NaOH. Absorbance was measured at 405 nm in a plate reader, and activity calculated from standard curve generated using p-nitrophenol standards. TRAP activity was normalized to total protein (determined using the Bradford assay (Bio-Rad protein assay catalog# 500–0006)) as well as to total number of nuclei counted after TRAP and hematoxylin staining of a second, identical 96-well plate run

in conjunction with that used for the TRAP assay.

RT-PCR

Primers for RT-PCR of IL-1R1 and IL-1R2 were generated from mouse sequences retrieved from Genbank. Primers used were as follows: IL-1R1 sense: 5′-gctctagacatagtgctttgg-tacaggga-3′; IL-1R1 antisense 5′-gacgtcgactca-tagtcttggattttctcc-3′; IL-1R2 sense: 5′-gctctag-atgaactgacctgaatgaattca-3′; IL-1R2 antisense 5′-gacgtcgactcccagaaacactttacacggga-3′ with annealing temperatures of 62 and 60°C, respectively. Primers and annealing temperatures for GAPDH, TRAP, and RANK are previously described in Haynes et al. [1999], Battaglino et al. [2002] and Mori et al. [2002], respectively. RNA was first DNase I treated according to the manufacturer's instructions (Invitrogen). Reverse transcription of 3 μg RNA was also carried out following instructions outlined by the manufacturer of Revert-aid H Minus First Strand cDNA synthesis kit (Fermentas). PCR reaction was then carried out using HotStar Taq (Qiagen) in 50 μl reaction volumes consisting of $1\times$ PCR buffer, 0.2 mM dNTPs, 0.5 μM of each primer, 1.5 mM $MgCl_2$ (2.5 mM for IL-1R1), 1.25 U HotStar Taq DNA polymerase and 5–7 μl of cDNA from the RT reaction. The PCR reaction was initiated at 95°C for 15 min, followed by 30–40 cycles of 94°C for 45 s, 60°C (or appropriate annealing temperature) for 1 min, 72°C for 1 min and ending with 72°C for 10 min for all reactions. Expected fragments 310 bp (RANK), 407 bp (IL-1R1), 307 bp (IL-1R2), 465 bp (TRAP), and ~280 bp (GAPDH) were run on 2% agarose gels at 75 V for ~1.5 h. Images were captured using GeneSnap (Syngene) followed by semi-quantification and analysis of band intensities normalized to GAPDH levels using GeneTools (Syngene).

Resorption Assay

Osteoclastic activity in the presence or absence of IL-1β (1 and 10 ng/ml) and/or IL-1ra (50 ng/ml) was assessed using either osteologic^{TM} or bone/dentin disks. Dentin slices were cut using a Diamond wire histosaw (Delaware Diamond Knives, Inc.) of ~200 nm thickness from dentin kindly provided by Dr. R. Harrison at the University of Toronto. Size separated OCs generated from RAW cells were plated onto resorbable disks in 96-well dishes and left to resorb for 48 h. Cells were then fixed,

TRAP stained and counted. Cells were removed from dentin slices using bleach and sonication, after which time, resorption pits were stained for 30 s to 1 min with 1% toluidine blue, washed in PBS and dried. Osteologic disks were stained as previously described [Voronov et al., 2005]. Analysis of resorption pits was carried out using OpenLab^{TM} Software (Improvision).

Statistics

Statistics were carried out using SPSS 12.0 for windows using the independent samples t-test. Results were considered statistically significant if $P < 0.05$.

RESULTS

c-fms mRNA Levels are Higher in Large OCs than in Small OCs

M-CSF is essential for OC differentiation into functional multinucleated cells and has also been linked to OC activity [Sherr et al., 1988; Lees and Heersche, 1999; Roodman, 1999; Boyle et al., 2003; Tanaka et al., 2003; Teitelbaum and Ross, 2003]. Therefore, the receptor for M-CSF, c-fms, was investigated as being a possible determinant for differences between large and small OCs.

Using ^{35}S-RNA sense and antisense probes in three sets of experiments, we demonstrated RNA expression in large and small OCs isolated from rabbit long bones. We found 107.8 ± 22.3 grains per nucleus in large OCs and 65 ± 5 grains per nucleus in small OCs, a 1.7-fold difference (Fig. 1A,B). No signal was obtained using the control sense probe (data not shown). These OC populations consist of cells containing anywhere from 3 to 25 nuclei. We selected two size categories, small (≤ 5 nuclei) and large (≥ 10 nuclei) to create two distinct non-overlapping categories [Lees and Heersche, 2000; Lees et al., 2001; Manolson et al., 2003]. To define OC size, the number of nuclei per OC rather than surface area, was selected since surface area does not necessarily relate to OC size because migrating OCs tend to be spread out while stationary OCs tend to have a more rounded shape [Lakkakorpi and Vaananen, 1996]. Moreover, cytoplasmic volume has been shown to correlate with nuclei number [Lakka-korpi and Vaananen, 1996]. We also observed that 7.5% of small OCs had >108 grains/nucleus which is the average number of grains/nucleus for large OCs. This correlates with our previous
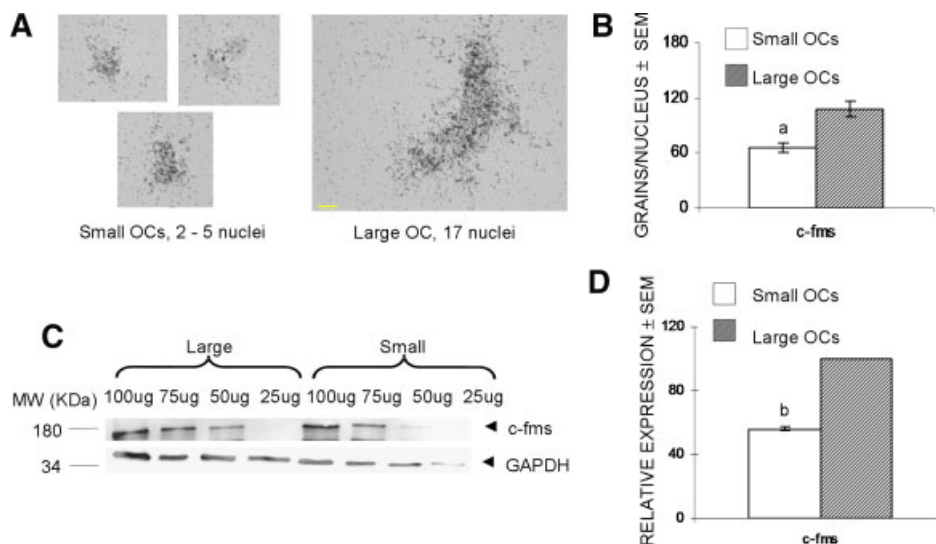
Fig. 1. c-fms mRNA and protein expression are higher in large compared to small OCs. **A**: In situ hybridization was performed on large and small rabbit long bone OCs with ^{35}S-labeled RNA probes to the M-CSF receptor, c-fms. **B**: Quantification of in situ hybridization was performed by counting individual grains in large (*striped bars*) and small (*white bars*) cells using Image-Pro Plus 4.1 software (Media Cybernetics, L.P.). To account for differences in cell size, results were normalized by expressing the number of grains per cell as grains per nucleus. Results are expressed as means ± the standard error. N = 40 for small, N = 15 for large OCs [a]$P < 0.01$ by unpaired, two tailed Student's *t*-test. Similar results are seen in repeated experiments. **C**: Whole cell extracts from enriched populations of large (Large) and small (Small) RAW-derived OCs were run on SDS–PAGE gels as a series of dilutions and immunoblotted as described in Materials and Methods. Results from a typical experiment are shown in subpart C. Similar results are seen with additional experiments. **D**: Immunoblots were quantified and normalized to GAPDH expression. Results were expressed as relative expression between large and small OCs, with expression of large OCs set at 100%. Numbers reflect the mean of three separate experiments in which populations of large (striped bars) and small (white bars) OCs were enriched as described in methods. [b]$P < 0.001$.

observation that the proportion of small OCs resorbing was approximately 6% [Lees et al., 2001].

In Large OCs Differentiated From RAW Cells c-fms Protein Expression is Higher Than in Small OCs

The number of OCs that can be obtained from rabbit long bones is insufficient for larger scale experiments. Therefore, the RAW cell line was used to generate large and small OCs as previously described in Manolson et al. [2003].

To validate the RAW cell system, we compared c-fms mRNA expression in authentic rabbit OCs with c-fms protein expression in OCs derived from RAW cells. Immunoblots (Fig. 1C,D) revealed c-fms protein expression was 1.8-fold higher in large OCs than in small OCs. Immunoblotting experiments were normalized to GAPDH levels, as it was previously shown that GAPDH mRNA and protein levels in the large and small OCs do not differ [Manolson et al., 2003]. This difference was similar to that observed with regard to mRNA expression in rabbit long bone OCs, suggesting that RAW derived OCs are comparable to authentic rabbit

OCs in this regard. Similarities between rabbit OCs and the RAW-derived OCs were also found previously for RNA and protein expression of the a3 V-ATPase subunit [Manolson et al., 2003]. Distinctions noted between the large and small OCs using this model system could result from differences in culture time rather than differences in size. To address this issue we compared results from size fractionated OCs to our current model.

Obtaining Enriched Populations of Large and Small OCs Either by Time of Differentiation or by Size Fractionation Yield Similar Results Showing that Interleukin-1 Receptors are Differentially Expressed in Large and Small OCs

Interleukin-1 (IL-1) is a predominant cytokine in inflammatory conditions such as rheumatoid arthritis and is also implicated in OC activation [Pacifici et al., 1991; Jimi et al., 1999; Dayer, 2003]. IL-1 is known to have two receptors, IL-1 receptor type I (IL-1R1) and IL-1 receptor type II (IL-1R2), of which IL-1R1 is the signaling (or activating) receptor and IL-1R2 is a decoy receptor unable to signal due to its lack of a cytoplasmic tail [Dinarello, 1998].

Immunoblotting of protein from enriched populations of large and small OCs at days 3–5 or days 5–8 respectively, revealed that IL-1R1 expression was 2-fold higher in large OCs ($P < 0.05$). Conversely, IL-1R2 was higher in small OCs by approximately 1.5-fold ($P < 0.01$) (Fig. 2A,B).

The distinctions noted between the large and small OCs could result from differences in culture time rather than differences in size. To address this issue, large and small OCs were obtained from RAW cells uniformly cultured for 5 days and size separated by a 40%/70% FBS step gradient (Fig. 2C,D). Replating OCs isolated from each gradient layer stained for TRAP and counted demonstrated that at least 80% of OCs obtained from a respective layer represented the population of interest (large OCs vs. small OCs) (Fig. 2D). Similar to the results shown in Figure 2B, IL-1R1 was 1.8-fold higher in large OCs compared to small OCs and

IL-1R2 was increased 1.5-fold in small OCs compared to large OCs (Fig. 2E,F). This shows that comparable results are obtained from enriched populations of large and small OCs irrespective of the fashion in which the populations were obtained. Considering the limited yield resulting from step gradient size fractionation and its labor-intensity, all subsequent studies on large and small OCs were carried out obtaining enriched populations after 5 and 8 days of culture.

Interleukin-1 Receptor RNA is Differentially Expressed in Large and Small OCs

To ask whether the differences in IL-1 receptor expression were transcriptionally or translationally regulated, RT-PCR was performed using mRNA isolated from large and small OCs. We found that RNA expression for IL-1R1 was 3-fold higher in large OCs compared to small OCs while the expression of
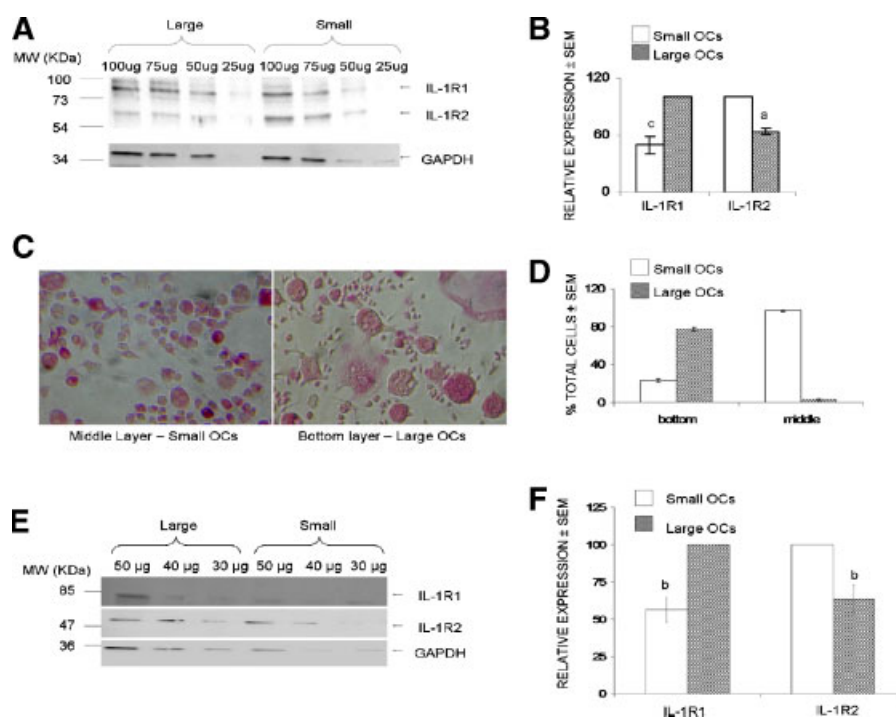

Fig. 2. Interleukin-1 Receptors are differentially expressed in OCs derived from enriched populations of large and small OCs. Protein extracts from enriched populations of large (Large) and small (Small) RAW-derived OCs isolated at day 5 or day 8 respectively were run on SDS–PAGE and immunoblotted as described in Materials and Methods. Results from a typical single experiment are reflected in subpart **A**. Similar results were obtained in other experiments. **B**: Numbers reflect the mean of three separate experiments. OCs grown in 200 ng/ml sRANKL for 5 days were separated according to size using gradient separation as described in Materials and Methods. Results from a typical single experiment are reflected in subparts **C**–**F**. C: Cells were replated and left in culture for 24 h and fixed, TRAP stained and counted. D: The number of cells counted were expressed as a percentage of total cells in the culture dish. E: Protein extracts from enriched populations of OCs obtained via gradient separation were run on SDS–PAGE gels and immunoblotted with antibodies to IL-1R1 and IL-1R2 as described in materials and methods. F: Immunoblots in subpart E were quantified and normalized to GAPDH. To compare between experiments, results were expressed as relative expression between large and small OCs, with expression of large OCs set at 100%. [c]$P < 0.05$, [a]$P < 0.01$. Numbers reflect the mean of three separate experiments.

IL-1R2 was 2.1-fold higher in small OCs compared to large OCs (Fig. 3A,B).

Interleukin-1 Preferentially Stimulates Resorptive Activity of Large OCs

Considering that large OCs had higher expression of the activating receptor, IL-1R1, and lower expression of the decoy receptor IL-1R2, and further considering that IL-1β is increased in inflammatory situations, we hypothesized that IL-1β would result in increased resorption by large OCs. To test this hypothesis, resorption assays were carried out on populations of large and small RAW-derived OCs isolated by FBS step gradients in the presence and absence of IL-1β and its antagonist IL-1ra. No differences in resorptive activity were noted in the absence of IL-1β. In the

Fig. 3. RNA for Interleukin-1 receptors IL-1R1 and IL-1R2 are differentially expressed between large and small OCs. **A:** RNA extracted from enriched populations of large (Large) and small (Small) RAW-derived OCs were subjected to RT-PCR as previously described. Results from a typical experiment are reflected in subpart A. Similar results were obtained from other experiments. **B:** PCR bands in subpart A were quantified and normalized to GAPDH. To compare between experiments, results were expressed as relative expression between large and small OCs, with expression of large OCs set at 100%. Numbers reflect the mean of three separate experiments. $^{c}P < 0.05$, $^{a}P < 0.01$.

presence of 1 ng/ml IL-1β, large OCs resorbed more area per OC (Fig. 4) and had a greater area per pit than small OCs (Fig. 4). This difference was eliminated by the additional presence of the IL-1 antagonist IL-1ra. Ten-fold higher concentrations of IL-1β (10 ng/ml) did not result in significant differences between large and small OCs suggesting that the higher levels of the decoy receptor IL-1R2 in the small OCs are being saturated. These results are consistent with our hypothesis that differential expression of IL-1R1 and IL-1R2 in large and small OCs result in a differential resorptive activity in response to extracellular factors.

Enzyme Markers of OC Activity are Higher in Large OCs

Expression of enzymes characteristic of and abundant in OCs such as the gelatinase Matrix Metalloproteinase-9 (MMP-9) and the cysteine protease Cathepsin K (CatK) [Delaisse et al., 2003] were higher in large OCs (Fig. 5C,D) than in small ones.

RNA expression for TRAP was similar in large and small OCs (Fig. 5A,B) and TRAP activity, used as an indirect measure of TRAP protein expression, also demonstrated no differences between large and small OCs when normalized to either total cell protein (Fig. 5E) or to the number of nuclei (data not shown).
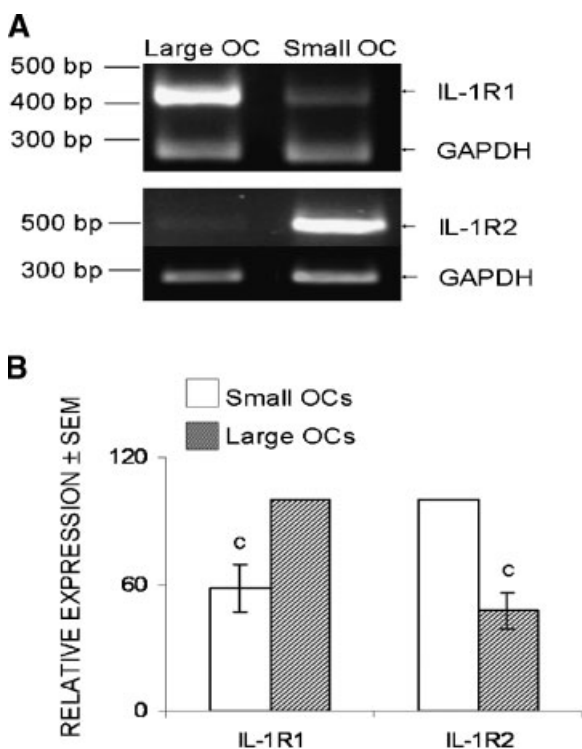
Receptors for Receptor Activator of Nuclear Factor kappa B Ligand (RANKL) and TNFα are More Highly Expressed in Large OCs than in Small Ones

We examined receptors for factors that have been shown to be important in OC activation. Two of these receptors, RANK and Tumor Necrosis Factor Receptor 1 (TNFR1), belong to the same protein superfamily [Boyle et al., 2003; Wittrant et al., 2003]. As shown in Figure 6C,D, both receptors are higher in large OCs than in small ones by approximately 2.5- and 2-fold for RANK and TNFR1 respectively. This was also true for RANK mRNA expression which was 2-fold higher in large OCs than in small ones (Fig. 6A,B).

Src Homology 2-containing Inositol-5-phosphatase (SHIP) protein Expression is Higher in Large OCs than in Small Ones

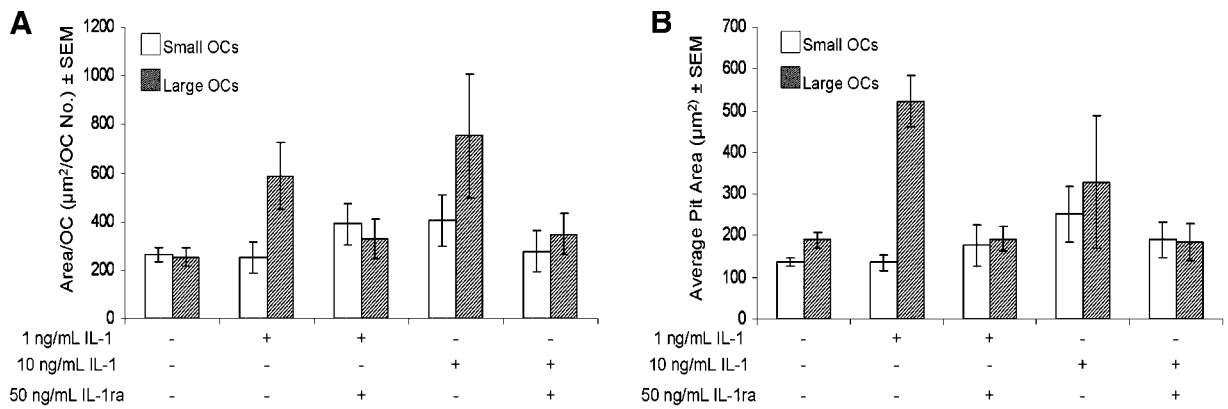Knockout of SHIP in mice was shown by Takeshita et al. [2002] to result in osteoporosis

Fig. 4. Interleukin-1β preferentially stimulates resorption by large OCs. OCs derived from RAW cells were size separated on an FBS step gradient into two populations of large and small osteoclasts as described in Materials and Methods. The two populations were then replated onto dentin disks and allowed to resorb for 48 h in the presence of IL-1β (1 and 10 ng/ml) and in the presence or absence of inhibitor IL-1ra (50 ng/ml). Osteoclasts were visualized and counted by TRAP staining and resorption pits were stained with toluidine blue and quantified using image analysis. The results are presented as mean ± standard error of the mean (n = 2). Similar results were obtained in two other experiments.
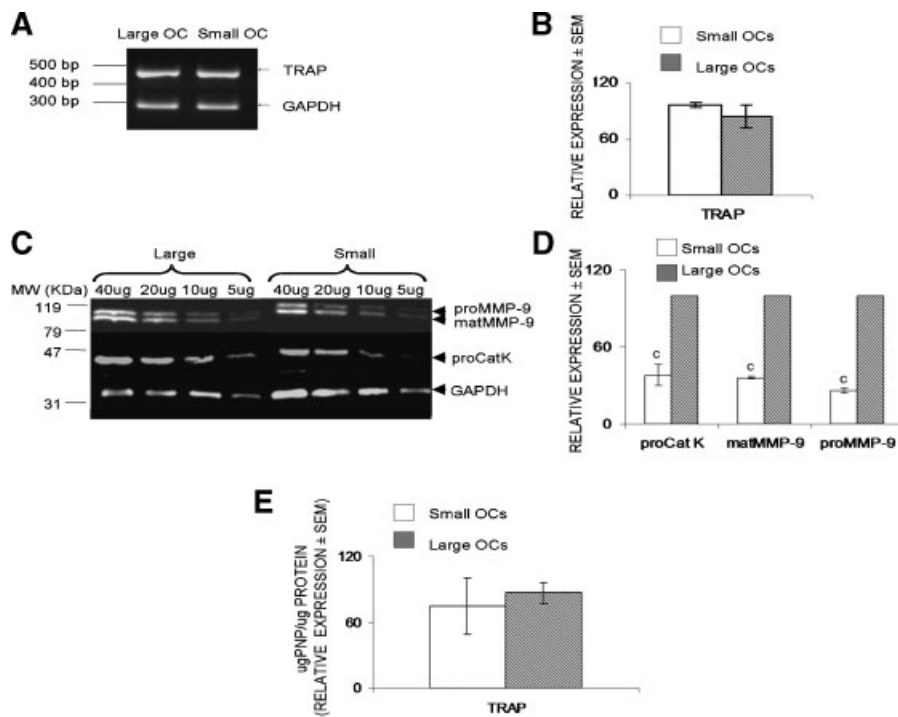

Fig. 5. Extracellular Proteases, cathepsin K and MMP-9, are increased in large compared to small OCs while TRAP expression and activity was not significantly different between the two populations. **A**, **B**: RNA from large and small OCs grown as previously described, was subjected to RT-PCR with primers to TRAP. Bands run on agarose gel were then quantified and normalized to GAPDH. To compare between experiments, results were expressed as relative expression between large and small OCs, with expression of large OCs set at 100%. Numbers reflect the mean of three separate experiments ± standard error of the mean. **C**: Protein extracts from enriched populations of large (Large) and small (Small) RAW-derived OCs were run on SDS-PAGE as described in Materials and Methods. Results from a typical experiment are shown in subpart C. Similar results were obtained in other experiments. **D**: Immunoblots in subpart C were quantified and normalized to GAPDH. To compare between experiments, results were expressed as relative expression between large and small OCs, with expression of large OCs set at 100%. Numbers reflect the mean of three separate experiments. $^{c}P < 0.05$. **E**: RAW-cell derived OCs grown in 96-well dishes for enriched populations of large and small OCs were assayed for TRAP enzyme activity (μg PNP) as described in Materials and Methods. TRAP activity was then normalized to total protein, expressed as μg PNP/μg protein and compared by relative expression with the higher activity set to 100%.
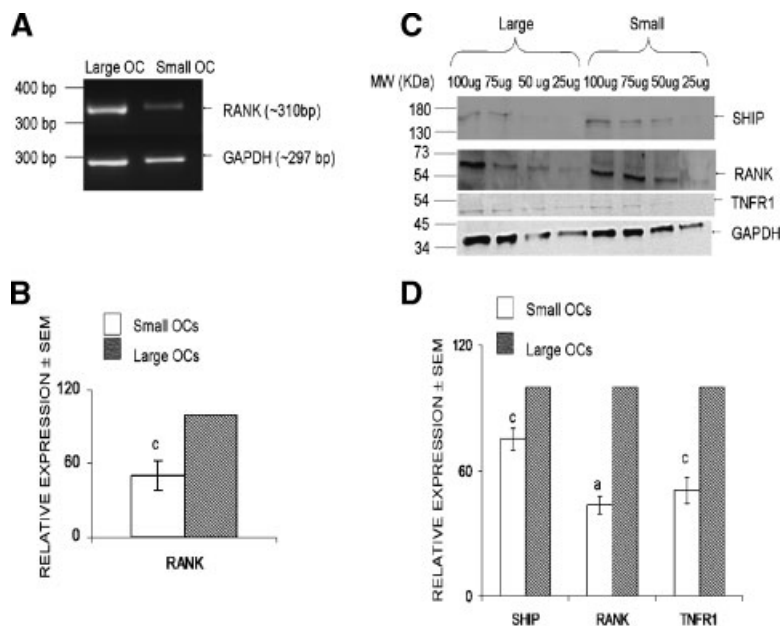
Fig. 6. Signaling molecule SHIP, as well as receptors for RANKL and TNFα, show higher expression in large OCs. **A**, **B**: RNA extracted from enriched populations of large (Large) and small (Small) RAW-derived OCs were subjected to RT-PCR. Results from a typical experiment are reflected in subpart A. B: PCR bands in subpart A were quantified and normalized to GAPDH. To compare between experiments, results were expressed as relative expression between large and small OCs, with expression of large OCs set at 100%. Numbers reflect the mean of three separate experiments. [a]$P < 0.01$, [c]$P < 0.05$. **C**: Protein extracts from enriched populations of large (Large) and small (Small) RAW-derived OCs were run on SDS–PAGE as a series of dilutions described in Materials and Methods. Results from a typical experiment are shown in subpart C, with similar results obtained in other experiments. **D**: Immunoblots in subpart C were quantified and normalized to GAPDH expression. To compare between experiments, results were expressed as relative expression between large and small OCs, with expression of large OCs set at 100%. Numbers reflect the mean of three separate experiments; [c]$P < 0.05$.

due to increased OC number and size and it was proposed that SHIP is a negative regulator of OC activation in the RANKL signaling pathway [Takeshita et al., 2002; Boyle et al., 2003; Kalesnikoff et al., 2003]. We therefore investigated the expression of this protein in large and small OCs. We found SHIP expression to be 1.3-fold higher in large OCs compared to small ones (Fig. 6C,D) ($P < 0.05$).

Integrin Components α_v and β_3 Expressions are both Higher in Large OCs Compared to Small Ones

Attachment of OCs to bone is required for resorption and occurs through integrins abundant in OCs. $\alpha_v\beta_3$ is the most abundant integrin in OCs and inhibition of $\alpha_v\beta_3$ inhibited OC bone resorption [Nakamura et al., 2003]. Evaluation of expression of the α_v subunit of this integrin in large and small OCs revealed a 2.2-fold increase in large OCs, while that of integrin subunit β_3 revealed a 4.5-fold increase in large OCs compared to small (Fig. 7A,B).

Expression of Fusion Receptor Signal-regulatory Peptide (SIRPα1) is Higher in Small OCs

OCs and macrophages are derived from the same lineage of cells [Vignery, 2000] and thus share many features. SIRPα1 is a receptor implicated in macrophage fusion, resulting in multinucleated giant cells [Saginario et al., 1995]. Vignery proposed SIRPα1 to have a similar role in OC fusion and found that mononuclear and small multinuclear osteoclastic cells express more SIRPα1 than larger OCs [Vignery, 2000]. They suggested that SIRPα1 expression was controlling OC fusion rates and OC size. We demonstrate here using immunoblot detection of SIRPα1, that this receptor is significantly increased in the small OCs compared to large OCs, with a noted 1.6-fold increase in small ($P < 0.05$) (Fig. 7A,B).

DISCUSSION

We have shown previously that large OCs as a population are more active resorbers than small OCs, and that the reason for this is that the
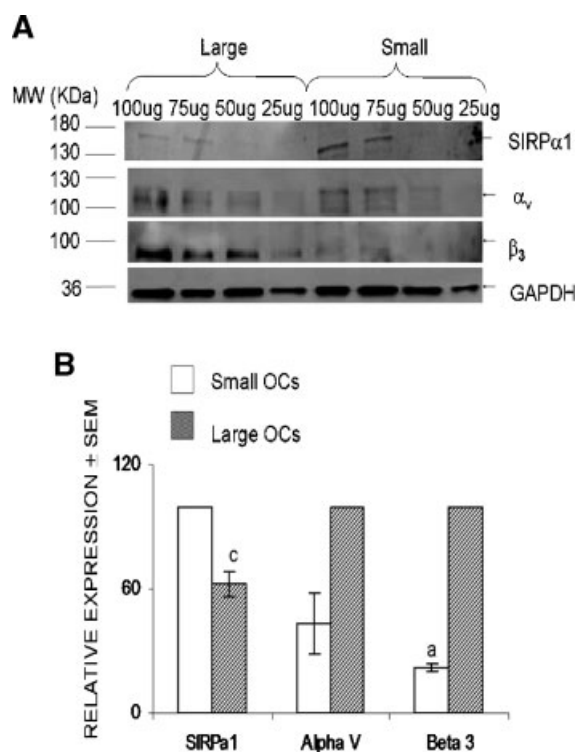
A

B

Fig. 7. Integrin subunits α_v and β_3 protein, as well as fusion receptor signal-regulatory peptide (SIRPα1) show increased expression in small compared to large OCs. **A**: Protein extracts from enriched populations of large (Large) and small (Small) RAW-derived OCs were run on SDS–PAGE as a series of dilutions and immunoblotted as described in Materials and Methods. Results from a single experiment are shown in subpart A, with similar results obtained in other experiments. **B**: Immunoblots in (A) were quantified and normalized to GAPDH. To compare between experiments, results are expressed as relative expression between large and small OCs, with expression of large OCs set at 100%. Numbers reflect three separate experiments. $^aP < 0.01$, $^cP < 0.05$.

proportion of large OCs in a resorptive state is greater (40%) than that of small OCs (6%) [Lees et al., 2001]. Here we tested the hypothesis that differences in resorptive activity could arise from differences in activation mechanisms evolving from different receptor expression levels in larger and smaller OCs. We found that the expression of activating receptors (c-fms, IL-1R1, TNFR1, RANK, integrins α_v, and β_3) and activity in response to IL-1β was higher in the larger OCs while the expression of inhibitory and fusion receptors (IL-1R2, SIRPα1) was lower in the large OCs.

We used isolated rabbit OCs and RAW cell derived OCs for our studies. Initial experiments were single cell assays carried out using OC populations obtained from the rabbit long

bones. To look for novel differences between large and small OCs using proteomic and genomic analysis it was necessary to obtain larger numbers of OCs. There are two published methods of obtaining enriched populations of OC-like cells in which at least 75% of the cells have ≤ 5 or ≥ 10 nuclei: RAW cells could be cultured for varying periods of time [Manolson et al., 2003], or alternatively, RAW cells could be cultured for a uniform time and then size separated using a 40%/70% FBS step gradient [Collin-Osdoby et al., 2003]. Both methods yielded similar results with respect to IL-1 receptor expression (Fig. 2). We defined small OCs as having 2–5 nuclei and large OCs as ≥ 10 nuclei to create non-overlapping categories of OCs [Lees and Heersche, 2000; Lees et al., 2001]. The fact that the numbers of large OCs increase with time in culture indicates that large and small OCs represent different stages of maturation. The same would be the case in vivo. The real question in vivo is why in certain areas large OCs predominate. This has likely to do with apoptosis since cytokines such as IL-1, TNFα and RANKL increased in these inflammatory states are pro-survival factors [Jimi et al., 1998; Glantschnig et al., 2003]. The fact remains we have shown before that large authentic rabbit OCs are more effective resorbers and display different levels of the ATPase subunit a3 expression; characteristics which were shown by Lees et al. [2001] [Manolson et al., 2003]. We have shown here, and previously [Manolson et al., 2003] that these differences are similar in rabbit OCs and RAW-cell derived OCs.

In the present series of experiments, we found similar differences between large and small rabbit OCs and large and small RAW-derived OCs. We found a 1.7-fold higher expression of c-fms mRNA expression in large versus small authentic rabbit OCs (Fig. 1) and a 1.8-fold higher expression of c-fms protein in large versus small RAW-derived OCs. Using the RAW-derived OCs, we found that large OCs also had higher expression levels of IL-1R1 while small OCs had higher expression levels of the decoy receptor, IL-1R2 (Figs. 2 and 3). Using an adjuvant arthritis rat model, Xu et al. [1996] found that OCs in normal bone express both IL-1R1 and IL-1R2, while OCs in arthritic bone primarily expressed the type I receptor. Assuming that based on the evidence by others [Aota et al., 1996] that OCs in arthritic bone are

larger [not reported by Xu et al., 1996], these results would be similar to ours. Our results also parallel those of Wei et al. [2005] who showed increased IL-1R1 RNA expression and decreased IL-1R2 expression in bone marrow macrophages differentiated over 4 days of exposure to RANKL.

We defined two categories of OCs based on the number of nuclei per cell (2–5 nuclei and ≥10 nuclei). We decided on this parameter rather than measuring cell size by surface area because OCs in the migratory phase are spread out, and have a large surface area whereas the same cell can assume a more rounded shape when stationary and then has a smaller surface area [Kanehisa and Heersche, 1988; Lakkakorpi and Vaananen, 1996]. As expected, when evaluated separately, the category of cells containing 6–9 nuclei had characteristics that were in between (results not shown).

To address whether the enzymes required for degrading the organic matrix of bone are also increased, the expression of the two most important OC proteinases, cathepsin K and MMP-9 was assessed. We found a 2- to 3-fold higher expression in large compared to small OCs (Fig. 5). Increased expression of MMP-9 may have broader implications regarding pathological bone loss since MMP-9 is thought to release TGF-β and ICAM and degrade IL-1β [Delaisse et al., 2003]. There is also data suggesting that MMPs generate collagen fragments that could activate OCs, possibly through the integrin $\alpha_v\beta_3$ [Holliday et al., 1997; Caldwell et al., 1998; Chiusaroli et al., 2003]. Finally, MMP-9 is thought to be associated with activation of the cytokines TNFα and IL-1 from inactive forms [McCawley and Matrisian, 2001; Nabeshima et al., 2002]. In each case, increased MMP-9 activity would be expected to increase osteoclastic activity beyond a corresponding linear increase in matrix degradation. Subsequently, increases in receptors TNFR1 and its related family member RANK may be a result of increased activation of these cytokines leading to increases in expression of their receptors [Komine et al., 2001; Kwan Tat et al., 2004].

Two proteins implicated in regulation of OC signaling and fusion, and therefore size, are SHIP and SIRPα1 and thus were obvious choices to explore. SHIP has been shown to be a negative regulator of the RANKL signaling pathway by dephosphorylating phosphatidylinositol-3,4,5-trisphosphate thereby blocking phosphatidylinositol-3-kinase-initiated signaling [Takeshita et al., 2002]. SHIP$^{-/-}$ OCs are hypersensitive to M-CSF and RANKL, are unusually large (containing up to 100 nuclei similar to pagetic OCs) and have increased resorptive activity resulting in severe osteoporotic SHIP$^{-/-}$ mice [Takeshita et al., 2002]. We hypothesized that the large OCs in our model system would express a lower amount of SHIP than the small OCs, but found instead a small but significant 1.3-fold higher expression in the large compared to small OCs (Fig. 6). These results suggest that SHIP expression may not be directly related to increased resorptive activity noted in inflammatory diseases. Rather, the slight increase in SHIP expression could be viewed as an attempt to downregulate the cell's response to signaling through the sRANKL/RANK pathway since our model does employ a high RANKL level.

We also found an increase in SIRPα1 in small compared to large RAW-derived OCs (Fig. 7), paralleling results obtained by Han et al. [2000], in rat alveolar macrophages. SIRPα1 (AKA p84/BIT/SHPS-1) has been implicated in macrophage fusion through interaction with CD47 [Han et al., 2000; Vignery, 2000; Seiffert et al., 2001; Liu et al., 2002; Oshima et al., 2002]. Vignery [2000] suggested that increased expression of this receptor on small OCs makes them more prone to fusion than larger OCs. Our results are compatible with this view.

The integrin $\alpha_v\beta_3$ is a key player in bone remodeling both through its direct involvement in regulating resorption and indirectly through transduction of inside-out and outside-in signals involved in OC differentiation, migration and apoptosis [Duong et al., 2000; van der Flier and Sonnenberg, 2001; Hynes, 2002]. Other integrins were also reported on OCs at lower levels such as: $\alpha_v\beta_1$ (vitronectin/fibronectin receptor), $\alpha_2\beta_1$ (collagen/laminin receptor) and $\alpha_v\beta_5$ [Nesbitt et al., 1993]. However, during osteoclastogenesis β_3 expression increases and associates with the α_v subunit resulting in increased $\alpha_v\beta_3$ expression [Boissy et al., 1998] and in their predominance over other integrins on the mature OC surface. Since the α_v subunit is found on OCs and pre-OCs associated with other integrin subunits and β_3 only appears after 2 days in culture [Boissy et al., 1998], with its expression is restricted to OCs, megakaryocytes, and platelets [Helfrich et al., 1992], it is

not surprising to see a dramatically higher β_3 expression (4.5-fold) compared to α_v (2.2-fold) in large OCs compared to small ones (Fig. 7). This suggests that β_3 is not only a marker of osteoclastogenesis, but provides some important functional/signaling role predominant in large and/or aggressively resorbing OCs. Interestingly, in another series of experiments not reported here, after treatment with an anti-$\alpha_v\beta_3$ blocking antibody [Wilder, 2002] large authentic rabbit OCs were less susceptible to detachment than small OCs (Gramoun et al, submitted), possibly as a result of the increased levels of integrin expression.

IL-1 has been shown to influence various signaling pathways within OCs [Troen, 2003; Blair et al., 2005] and various cytokine levels in vivo that affect OC function (i.e., TNF and RANKL [Nukaga et al., 2004; O'Gradaigh et al., 2004]). To this end, we asked if differences in the expression level of IL-1 receptors or differences in OC response to IL-1 exist. Immunoblotting demonstrated increased levels of IL-1R1 in large OCs and IL-1R2 in small OCs (Fig. 2). RT-PCR further revealed that the increases in receptor levels were mirrored by increases in mRNA suggesting transcriptional regulation (Fig. 3). It has been shown recently that in mouse bone marrow macrophages, RNA expression of the IL-1 receptors during osteoclastogenesis is influenced by prolonged exposure to RANKL [Wei et al., 2005] in that RANKL decreased IL-1R2 expression and increased IL-1R1 expression in 4 days of culture. Furthermore, as previously mentioned, differential IL-1 receptor expression has been noted in OCs derived from arthritic and osteoporotic females with pathological OCs primarily expressing IL-1R1 RNA [Xu et al., 1996; Sunyer et al., 1999].

Few IL-1 receptors need to bind IL-1 to initiate IL-1 signaling events. Furthermore, IL-1 receptor expression is generally low (reviewed in Dinarello [1996]). Considering this, we hypothesized that the 1.5- to 3-fold changes we noted in IL-1 receptor levels between large and small OCs could result in substantial alterations to resorptive activity in response to identical extracellular stimulants. We sought to test this hypothesis by assaying the changes in the resorptive capacity of large and small OCs to IL-l and its antagonist.

Supporting our hypothesis, we found that large OCs were indeed more responsive to low concentrations of IL-1β and that this increased activity was suppressed by the antagonist IL-1ra. Although the number of pits were equal (data not shown), large OCs resorbed more bone per OCs, with each resorption pit having a larger surface area than small OCs in response to 1 ng/ml IL-1β (Fig. 4). This increased activity was suppressed by 50 ng/ml IL-1ra.

Although small OC did not respond to 1 ng/ml, they did have a small increase in activity to 10 ng/ml IL-1β. This likely results from the 1.5-fold higher concentration of IL-1R2 on small OCs as it would necessitate higher concentrations of IL-1β to saturate the decoy receptors.

Considering the differences in RANK expression between large and small OCs one might also expect sRANKL to result in similar differences in resorption. Nevertheless, the presence of 50 ng/ml sRANKL in similar resorption assays did not result in any significant differences (data not shown). Instead the addition of sRANKL resulted in further differentiation and fusion of OCs in the cultures, minimizing the differences between the two groups.

Lees et al. [2001] showed similar resorptive differences between large and small OCs using a rabbit co-culture system. The differences in activity were not in response to a specific exogenous factor added to culture, but rather to a variety of factors produced by the accompanying stromal cells. In contrast, using OCs derived from RAW cells we did not see any differences in resorptive activity between the two populations without the addition of a stimulant to the culture system (i.e., IL-1β).

As mentioned previously, large OCs are more prevalent in sites of bone loss resulting from inflammatory diseases. The increase in OC size likely results from the increased level of sRANKL and other inflammatory cytokines, which in turn results from the increased presence of inflammatory cells [Kong et al., 1999]. Here we show that as size increases, so do the levels of activating receptors (IL-1R1, c-fms, RANK, TNFR1), which in turn, makes the OC hyperresponsive to exogenous signals. This "vicious cycle" may explain the pathological bone loss prevalent in many inflammatory conditions [Takayanagi, 2005; Sato and Takayanagi, 2006]. Current therapeutics inhibiting action of cytokines such as IL-1, TNFα and RANKL have proven effective in decreasing

bone erosion in pathological diseases such as inflammatory arthritis [Feldmann et al., 1996; Dayer, 2002; Bezerra et al., 2005]. An ideal antiresorptive therapeutic agent would reduce pathological resorption while maintaining the normal remodeling activity that is required for sustaining bone integrity. The heterogeneity in receptor expression between large and small OCs shown here could provide the groundwork for designing methods for selective inhibition and/or destruction of the most active OCs.

ACKNOWLEDGMENTS

REFERENCES

Aota S, Nakamura T, Suzuki K, Tanaka Y, Okazaki Y, Segawa Y, Miura M, Kikuchi S. 1996. Effects of indomethacin administration on bone turnover and bone mass in adjuvant-induced arthritis in rats. Calcif Tissue Int 59:385–391.

Arend WP, Dayer JM. 1990. Cytokines and cytokine inhibitors or antagonists in rheumatoid arthritis. Arthritis Rheum 33:305–315.

Battaglino R, Kim D, Fu J, Vaage B, Fu XY, Stashenko P. 2002. c-myc is required for osteoclast differentiation. J Bone Miner Res 17:763–773.

Bezerra MC, Carvalho JF, Prokopowitsch AS, Pereira RM. 2005. RANK, RANKL and osteoprotegerin in arthritic bone loss. Braz J Med Biol Res 38:161–170.

Blair HC, Robinson LJ, Zaidi M. 2005. Osteoclast signalling pathways. Biochem Biophys Res Commun 328:728–738.

Boissy P, Machuca I, Pfaff M, Ficheux D, Jurdic P. 1998. Aggregation of mononucleated precursors triggers cell surface expression of alpha$_v$beta$_3$ integrin, essential to formation of osteoclast-like multinucleated cells. J Cell Sci 111(Pt 17):2563–2574.

Boyle WJ, Simonet WS, Lacey DL. 2003. Osteoclast differentiation and activation. Nature 423:337–342.

Caldwell CB, Moran EL, Bogoch ER. 1998. Fractal dimension as a measure of altered trabecular bone in experimental inflammatory arthritis. J Bone Miner Res 13:978–985.

Chiusaroli R, Maier A, Knight MC, Byrne M, Calvi LM, Baron R, Krane SM, Schipani E. 2003. Collagenase cleavage of type I collagen is essential for both basal and parathyroid hormone (PTH)/PTH-related peptide receptor-induced osteoclast activation and has differential effects on discrete bone compartments. Endocrinology 144:4106–4116.

Collin-Osdoby P, Yu X, Zheng H, Osdoby P. 2003. RANKL-mediated osteoclast formation from murine RAW 264.7 cells. Methods Mol Med 80:153–166.

Dayer JM. 2002. The saga of the discovery of IL-1 and TNF and their specific inhibitors in the pathogenesis and treatment of rheumatoid arthritis. Joint Bone Spine 69:123–132.

Dayer JM. 2003. The pivotal role of interleukin-1 in the clinical manifestations of rheumatoid arthritis. Rheumatology (Oxford) 42(Suppl 2):ii3–ii10.

Delaisse JM, Andersen TL, Engsig MT, Henriksen K, Troen T, Blavier L. 2003. Matrix metalloproteinases (MMP) and cathepsin K contribute differently to osteoclastic activities. Microsc Res Tech 61:504–513.

Dinarello CA. 1996. Biologic basis for interleukin-1 in disease. Blood 87:2095–2147.

Dinarello CA. 1998. Interleukin-1, interleukin-1 receptors and interleukin-1 receptor antagonist. Int Rev Immunol 16:457–499.

Duong LT, Lakkakorpi P, Nakamura I, Rodan GA. 2000. Integrins and signaling in osteoclast function. Matrix Biol 19:97–105.

Feldmann M, Brennan FM, Maini RN. 1996. Role of cytokines in rheumatoid arthritis. Annu Rev Immunol 14:397–440.

Glantschnig H, Fisher JE, Wesolowski G, Rodan GA, Reszka AA. 2003. M-CSF, TNFalpha and RANK ligand promote osteoclast survival by signaling through mTOR/S6 kinase. Cell Death Differ 10:1165–1177.

Ha H, Kwak HB, Lee SK, Na DS, Rudd CE, Lee ZH, Kim HH. 2003. Membrane rafts play a crucial role in receptor activator of nuclear factor kappaB signaling and osteoclast function. J Biol Chem 278:18573–18580.

Han X, Sterling H, Chen Y, Saginario C, Brown EJ, Frazier WA, Lindberg FP, Vignery A. 2000. CD47, a ligand for the macrophage fusion receptor, participates in macrophage multinucleation. J Biol Chem 275:37984–37992.

Haynes DR, Atkins GJ, Loric M, Crotti TN, Geary SM, Findlay DM. 1999. Bidirectional signaling between stromal and hemopoietic cells regulates interleukin-1 expression during human osteoclast formation. Bone 25:269–278.

Helfrich MH, Nesbitt SA, Horton MA. 1992. Integrins on rat osteoclasts: Characterization of two monoclonal antibodies (F4 and F11) to rat beta 3. J Bone Miner Res 7:345–351.

Holliday L, Welgus H, Fliszar C, Veith G, Jeffrey J, Gluck S. 1997. Initiation of osteoclast bone resorption by interstitial collagenase. J Biol Chem 272:22053–22058.

Hynes RO. 2002. Integrins: Bidirectional, allosteric signaling machines. Cell 110:673–687.

Jimi E, Nakamura I, Ikebe T, Akiyama S, Takahashi N, Suda T. 1998. Activation of NF-kappaB is involved in the survival of osteoclasts promoted by interleukin-1. J Biol Chem 273:8799–8805.

Jimi E, Nakamura I, Duong LT, Ikebe T, Takahashi N, Rodan GA, Suda T. 1999. Interleukin 1 induces multinucleation and bone-resorbing activity of osteoclasts in

the absence of osteoblasts/stromal cells. Exp Cell Res 247:84–93.

Kalesnikoff J, Sly LM, Hughes MR, Buchse T, Rauh MJ, Cao LP, Lam V, Mui A, Huber M, Krystal G. 2003. The role of SHIP in cytokine-induced signaling. Rev Physiol Biochem Pharmacol 149:87–103.

Kanehisa J, Heersche JN. 1988. Osteoclastic bone resorption: In vitro analysis of the rate of resorption and migration of individual osteoclasts. Bone 9:73–79.

Komine M, Kukita A, Kukita T, Ogata Y, Hotokebuchi T, Kohashi O. 2001. Tumor necrosis factor-alpha cooperates with receptor activator of nuclear factor kappaB ligand in generation of osteoclasts in stromal cell-depleted rat bone marrow cell culture. Bone 28:474–483.

Kong YY, Feige U, Sarosi I, Bolon B, Tafuri A, Morony S, Capparelli C, Li J, Elliott R, McCabe S, Wong T, Campagnuolo G, Moran E, Bogoch ER, Van G, Nguyen LT, Ohashi PS, Lacey DL, Fish E, Boyle WJ, Penninger JM. 1999. Activated T cells regulate bone loss and joint destruction in adjuvant arthritis through osteoprotegerin ligand [In Process Citation]. Nature 402:304–309.

Kwan Tat S, Padrines M, Theoleyre S, Heymann D, Fortun Y. 2004. IL-6, RANKL, TNF-alpha/IL-1: Interrelations in bone resorption pathophysiology. Cytokine Growth Factor Rev 15:49–60.

Lakkakorpi PT, Vaananen HK. 1996. Cytoskeletal changes in osteoclasts during the resorption cycle. Microsc Res Tech 33:171–181.

Lees RL, Heersche JN. 1999. Macrophage colony stimulating factor increases bone resorption in dispersed osteoclast cultures by increasing osteoclast size. J Bone Miner Res 14:937–945.

Lees RL, Heersche JN. 2000. Differences in regulation of pH(i) in large ($\geq$10 nuclei) and small ($\leq$5 nuclei) osteoclasts. Am J Cell Physiol 279:C751–C761.

Lees RL, Sabharwal VK, Heersche JN. 2001. Resorptive state and cell size influence intracellular pH regulation in rabbit osteoclasts cultured on collagen-hydroxyapatite films. Bone 28:187–194.

Liu Y, Buhring HJ, Zen K, Burst SL, Schnell FJ, Williams IR, Parkos CA. 2002. Signal regulatory protein (SIRPalpha), a cellular ligand for CD47, regulates neutrophil transmigration. J Biol Chem 277:10028–10036.

Manolson MF, Yu H, Chen W, Yao Y, Li K, Lees RL, Heersche JN. 2003. The a3 isoform of the 100-kDa V-ATPase subunit is highly but differentially expressed in large ($>$/=10 nuclei) and small ($<$/=5 nuclei) osteoclasts. J Biol Chem 278:49271–49278.

McCawley LJ, Matrisian LM. 2001. Matrix metalloproteinases: They're not just for matrix anymore! Curr Opin Cell Biol 13:534–540.

Mori H, Kitazawa R, Mizuki S, Nose M, Maeda S, Kitazawa S. 2002. RANK ligand, RANK, and OPG expression in type II collagen-induced arthritis mouse. Histochem Cell Biol 117:283–292.

Nabeshima K, Inoue T, Shimao Y, Sameshima T. 2002. Matrix metalloproteinases in tumor invasion: Role for cell migration. Pathol Int 52:255–264.

Nakamura I, Rodan GA, Duongle T. 2003. Regulatory mechanism of osteoclast activation. J Electron Microsc (Tokyo) 52:527–533.

Nesbitt S, Nesbit A, Helfrich M, Horton M. 1993. Biochemical characterization of human osteoclast integrins. Osteoclasts express alpha v beta 3, alpha 2 beta 1, and alpha v beta 1 integrins. J Biol Chem 268:16737–16745.

Nordstrom T, Shrode LD, Rotstein OD, Romanek R, Goto T, Heersche JN, Manolson MF, Brisseau GF, Grinstein S. 1997. Chronic extracellular acidosis induces plasmalemmal vacuolar type H+ ATPase activity in osteoclasts. J Biol Chem 272:6354–6360.

Nukaga J, Kobayashi M, Shinki T, Song H, Takada T, Takiguchi T, Kamijo R, Hasegawa K. 2004. Regulatory effects of interleukin-1beta and prostaglandin E2 on expression of receptor activator of nuclear factor-kappaB ligand in human periodontal ligament cells. J Periodontol 75:249–259.

O'Gradaigh D, Ireland D, Bord S, Compston JE. 2004. Joint erosion in rheumatoid arthritis: Interactions between tumour necrosis factor alpha, interleukin 1, and receptor activator of nuclear factor kappaB ligand (RANKL) regulate osteoclasts. Ann Rheum Dis 63:354–359.

Oshima K, Ruhul Amin AR, Suzuki A, Hamaguchi M, Matsuda S. 2002. SHPS-1, a multifunctional transmembrane glycoprotein. FEBS Lett 519:1–7.

Pacifici R, Carano A, Santoro SA, Rifas L, Jeffrey JJ, Malone JD, McCracken R, Avioli LV. 1991. Bone matrix constituents stimulate interleukin-1 release from human blood mononuclear cells. J Clin Invest 87:221–228.

Piper K, Boyde A, Jones SJ. 1992. The relationship between the number of nuclei of an osteoclast and its resorptive capability in vitro. Anat Embryol 186:291–299.

Roodman GD. 1999. Cell biology of the osteoclast. Exp Hematol 27:1229–1241.

Saginario C, Qian HY, Vignery A. 1995. Identification of an inducible surface molecule specific to fusing macrophages. Proc Natl Acad Sci USA 92:12210–12214.

Sato K, Takayanagi H. 2006. Osteoclasts, rheumatoid arthritis, and osteoimmunology. Curr Opin Rheumatol 18:419–426.

Seiffert M, Brossart P, Cant C, Cella M, Colonna M, Brugger W, Kanz L, Ullrich A, Buhring HJ. 2001. Signal-regulatory protein alpha (SIRPalpha) but not SIRPbeta is involved in T-cell activation, binds to CD47 with high affinity, and is expressed on immature CD34(+)CD38(−) hematopoietic cells. Blood 97:2741–2749.

Sherr CJ, Roussel MF, Rettenmier CW. 1988. Colony-stimulating factor-1 receptor (c-fms). J Cell Biochem 38:179–187.

Singer F, Roodman GD. 1996. Paget's disease of bone. In: Bilezikian J, LG R, GA R, editors. Principles of bone biology. San Diego: Academic Press. pp 969–977.

Smith MD, Triantafillou S, Parker A, Youssef PP, Coleman M. 1997. Synovial membrane inflammation and cytokine production in patients with early osteoarthritis. J Rheumatol 24:365–371.

Sunyer T, Lewis J, Collin-Osdoby P, Osdoby P. 1999. Estrogen's bone-protective effects may involve differential IL-1 receptor regulation in human osteoclast-like cells. J Clin Invest 103:1409–1418.

Takayanagi H. 2005. Inflammatory bone destruction and osteoimmunology. J Periodontal Res 40:287–293.

Takeshita S, Namba N, Zhao JJ, Jiang Y, Genant HK, Silva MJ, Brodt MD, Helgason CD, Kalesnikoff J, Rauh MJ, Humphries RK, Krystal G, Teitelbaum SL, Ross FP. 2002. SHIP-deficient mice are severely osteoporotic due to increased numbers of hyper-resorptive osteoclasts. Nat Med 8:943–949.

Tanaka S, Nakamura I, Inoue J, Oda H, Nakamura K. 2003. Signal transduction pathways regulating osteoclast differentiation and function. J Bone Miner Metab 21:123–133.

Teitelbaum SL, Ross FP. 2003. Genetic regulation of osteoclast development and function. Nat Rev Genet 4:638–649.

Troen BR. 2003. Molecular mechanisms underlying osteoclast formation and activation. Exp Gerontol 38:605–614.

van der Flier A, Sonnenberg A. 2001. Function and interactions of integrins. Cell Tissue Res 305:285–298.

Vignery A. 2000. Osteoclasts and giant cells: Macrophage-macrophage fusion mechanism. Int J Exp Pathol 81:291–304.

Voronov I, Heersche JN, Casper RF, Tenenbaum HC, Manolson MF. 2005. Inhibition of osteoclast differentiation by polycyclic aryl hydrocarbons is dependent on cell density and RANKL concentration. Biochem Pharmacol 70:300–307.

Wei S, Kitaura H, Zhou P, Ross FP, Teitelbaum SL. 2005. IL-1 mediates TNF-induced osteoclastogenesis. J Clin Invest 115:282–290.

Wilder RL. 2002. Integrin alphav beta3 as a target for treatment of rheumatoid arthritis and related rheumatic diseases. Ann Rheum Dis 61(Suppl 2):ii96–ii99.

Wittrant Y, Theoleyre S, Couillaud S, Dunstan C, Heymann D, Redini F. 2003. Regulation of osteoclast protease expression by RANKL. Biochem Biophys Res Commun 310:774–778.

Xu LX, Kukita T, Nakano Y, Yu H, Hotokebuchi T, Kuratani T, Iijima T, Koga T. 1996. Osteoclasts in normal and adjuvant arthritis bone tissues express the mRNA for both type I and II interleukin-1 receptors. Lab Invest 75:677–687.